Hybridisable discontinous Galerkin for second-order eliptic problems

Problem formulation

Consider the domain $\Omega = [0,1]^2$ such that $\partial\Omega = \Gamma_D \cup \Gamma_N \cup \Gamma_R$ with $\Gamma_D \cap \Gamma_N = \emptyset$, $\Gamma_D \cap \Gamma_R = \emptyset$ and $\Gamma_N \cap \Gamma_R = \emptyset$. More precisely, set

$$
\begin{aligned}
\Gamma_N &:= \left\{(x,y) \in \mathbb{R}^2 \quad : \quad y = 0\right\},\\
\Gamma_R &:= \left\{(x,y) \in \mathbb{R}^2 \quad : \quad x = 0\right\},\\
\Gamma_N &:= \partial\Omega \setminus (\Gamma_N \cup \Gamma_R),
\end{aligned}
$$

The following second-order linear scalar partial differential equation is defined

$$
\begin{cases}
-\boldsymbol{\nabla} \cdot (\kappa \boldsymbol{\nabla} u) = s & \text{in } \Omega,\\
u = u_D & \text{on } \Gamma_D,\\
\boldsymbol{n} \cdot (\kappa \boldsymbol{\nabla} u) = t & \text{on } \Gamma_N,\\
\boldsymbol{n} \cdot (\kappa \boldsymbol{\nabla} u) + \gamma u = g & \text{on } \Gamma_R.
\end{cases}
\tag{1}
$$

where κ and γ are the diffusion and convection coefficients, respectively, $\boldsymbol{n}$ is the outward unit normal vector to the boundary, s is a volumetric source term and u_D, t and g are the Dirichlet, Neumann and Robin data imposed on the corresponding portions of the boundary $\partial\Omega$.

1. Write the HDG formulation of the problem (1). More precisely, derive the HDG strong and weak forms of the local and global problems. [*Hint: the hybrid variable $\hat{u}$ needs to be introduced on both on Γ_N and Γ_R*]

We start with the defining the strong form in the broken computational domain as

$$
\begin{cases}
-\boldsymbol{\nabla} \cdot (\kappa \boldsymbol{\nabla} u) = s & \text{in } \Omega,\\
u = u_D & \text{on } \Gamma_D,\\
\boldsymbol{n} \cdot (\kappa \boldsymbol{\nabla} u) = t & \text{on } \Gamma_N,\\
\boldsymbol{n} \cdot (\kappa \boldsymbol{\nabla} u) + \gamma u = g & \text{on } \Gamma_R\\
[\![u\boldsymbol{n}]\!] = \boldsymbol{0} & \text{on } \Gamma,\\
[\![\boldsymbol{n} \cdot (\kappa \boldsymbol{\nabla} u)]\!] = 0 & \text{on } \Gamma,
\end{cases}
\tag{2}
$$

where $[\![\cdot]\!]$ denotes the jump operator. According to the classical formulation of the HDG the problem formulated in (2) can be solved in two phases. In the first step the problem is reduced to a local element-by-element formulation, which is denoted as follows

$$\begin{cases} \nabla \cdot \boldsymbol{q}_i = s & \text{in } \Omega_i, \\ \boldsymbol{q}_i + (\kappa \nabla u_i) = \mathbf{0} & \text{in } \Omega_i, \\ u_i = u_D & \text{on } \partial\Omega_i \cap \Gamma_D, \\ u_i = \hat{u} & \text{on } \partial\Omega_i \setminus \Gamma_D. \end{cases} \tag{3}$$

As a second step a global problem of the form

$$\begin{cases} [\![u\boldsymbol{n}]\!] = \mathbf{0} & \text{on } \Gamma, \\ [\![\boldsymbol{n} \cdot \boldsymbol{q}]\!] = 0 & \text{on } \Gamma, \\ \boldsymbol{n} \cdot \boldsymbol{q} = -t & \text{on } \Gamma_N, \\ -\boldsymbol{n} \cdot \boldsymbol{q} + \gamma \hat{u} = g & \text{on } \Gamma_R. \end{cases} \tag{4}$$

has to be solved to find $\hat{u}$ where $\boldsymbol{q} = -(\kappa \nabla u)$. It corresponds to the application of Neumann and Robin boundary conditions, as well as the transmission conditions. The first equation is already imposed in the local problem (3), which leads to the simplified form of the global problem:

$$\begin{cases} [\![\boldsymbol{n} \cdot \boldsymbol{q}]\!] = 0 & \text{on } \Gamma, \\ \boldsymbol{n} \cdot \boldsymbol{q} = -t & \text{on } \Gamma_N, \\ -\boldsymbol{n} \cdot \boldsymbol{q} + \gamma \hat{u} = g & \text{on } \Gamma_R. \end{cases} \tag{5}$$

Before continuing with the weak forms the following vector spaces are defined:

$$\begin{aligned} \boldsymbol{\mathcal{W}}(D) &= \left\{ \boldsymbol{w} \in [\mathcal{H}^1(D)]^{\mathtt{n_{sd}}}, D \subset \Omega \right\}, \\ \mathcal{V}(D) &= \left\{ v \in \mathcal{H}^1(D), D \subset \Omega \right\}, \\ \mathcal{M}(D) &= \left\{ \mu \in \mathcal{L}_2(S), S \subset \Gamma \cup \partial\Omega \right\}. \end{aligned}$$

In order to get the weak form of the local problem (3), $(\boldsymbol{q}_i, u_i) \in \boldsymbol{\mathcal{W}}(\Omega_i) \times \mathcal{V}(\Omega_i)$ has to be found for $i = 1, ..., \mathtt{n_{el}}$, given u_d on Γ_D and $\hat{u}$ on $\Gamma \cup \Gamma_N \cup \Gamma_R$ satisfying

$$\begin{aligned} -(\nabla v, \boldsymbol{q}_i)_{\Omega_i} + < v, \boldsymbol{n}_i \cdot \widehat{\boldsymbol{q}}_i >_{\partial\Omega_i} &= (v, s)_{\Omega_i}, \\ -(\boldsymbol{w}, \boldsymbol{q}_i)_{\Omega_i} + (\nabla \cdot \boldsymbol{w}, u_i)_{\Omega_i} &= < \boldsymbol{n}_i \cdot \boldsymbol{w}, u_D >_{\partial\Omega_i \cap \Gamma_D} + < \boldsymbol{n}_i \cdot \boldsymbol{w}, \hat{u} >_{\partial\Omega_i \setminus \Gamma_D}, \end{aligned}$$

for all $(\boldsymbol{w}, v) \in \boldsymbol{\mathcal{W}}(\Omega_i) \times \mathcal{V}(\Omega_i)$. The numerical fluxes $\widehat{\boldsymbol{q}}_i$ are defined for $i = 1, ..., \mathtt{n_{el}}$ as

$$\boldsymbol{n}_i \cdot \widehat{\boldsymbol{q}}_i := \begin{cases} \boldsymbol{n}_i \cdot \boldsymbol{q}_i + \tau_i (u_i - u_D) & \text{on } \partial\Omega_i \cap \Gamma_D, \\ \boldsymbol{n}_i \cdot \boldsymbol{q}_i + \tau_i (u_i - \hat{u}) & \text{elsewhere.} \end{cases} \tag{6}$$

With this definition of the numerical fluxes the weak problem now states: for $i = 1, ..., \mathtt{n_{el}}$ find $(\boldsymbol{q}_i, u_i) \in \boldsymbol{\mathcal{W}}(\Omega_i) \times \mathcal{V}(\Omega_i)$ while

$$\begin{aligned} < v, \tau_i u_i >_{\partial\Omega_i} - (\nabla v, \boldsymbol{q}_i)_{\Omega_i} + < v, \boldsymbol{n}_i \cdot \boldsymbol{q}_i >_{\partial\Omega_i} & \\ = (v, s)_{\Omega_i} + < v, \tau_i u_D >_{\partial\Omega \cap \Gamma_D} + < v, \tau_i \hat{u} >_{\partial\Omega_i \setminus \Gamma_D}, & \\ -(\boldsymbol{w}, \boldsymbol{q}_i)_{\Omega_i} + (\nabla \cdot \boldsymbol{w}, u_i)_{\Omega_i} = < \boldsymbol{n}_i \cdot \boldsymbol{w}, u_D >_{\partial\Omega_i \cap \Gamma_D} + < \boldsymbol{n}_i \cdot \boldsymbol{w}, \hat{u} >_{\partial\Omega_i \setminus \Gamma_D}, & \end{aligned} \tag{7}$$

is satisfied for all $(\boldsymbol{w}, v) \in \boldsymbol{\mathcal{W}}(\Omega_i) \times \mathcal{V}(\Omega_i)$.

The weak form of the global problem (5) can be stated as follows: find $\hat{u} \in \mathcal{M}(\Gamma \cup \Gamma_N \cup \Gamma_R)$ for all $\mu \in \mathcal{M}(\Gamma \cup \Gamma_N \cup \Gamma_R)$ such that

$$\sum_{i=1}^{\mathtt{n_{el}}} < \mu, \boldsymbol{n}_i \cdot \widehat{\boldsymbol{q}}_i >_{\partial\Omega_i \setminus \Gamma} + \sum_{i=1}^{\mathtt{n_{el}}} < \mu, \boldsymbol{n}_i \cdot \widehat{\boldsymbol{q}}_i + t >_{\partial\Omega_i \cup \Gamma_N} + \sum_{i=1}^{\mathtt{n_{el}}} < \mu, \boldsymbol{n}_i \cdot \widehat{\boldsymbol{q}}_i - \gamma\hat{u} + g >_{\partial\Omega_i \cup \Gamma_R} = 0.$$

With the given definition of the numerical fluxes the global weak problem is defined as: find $\hat{u} \in \mathcal{M}(\Gamma \cup \Gamma_N \cup \Gamma_R)$ for all $\mu \in \mathcal{M}(\Gamma \cup \Gamma_N \cup \Gamma_R)$ such that

$$\begin{aligned} \sum_{i=1}^{\mathtt{n_{el}}} \Big\{ < \mu, \tau_i u_i >_{\partial\Omega_i \setminus \Gamma_D} + < \mu, \boldsymbol{n}_i \cdot \boldsymbol{q}_i >_{\partial\Omega_i \setminus \Gamma_D} - < \mu, \tau_i \hat{u} >_{\partial\Omega_i \setminus \Gamma_D} - < \mu, \gamma\hat{u} >_{\partial\Omega_i \cap \Gamma_R} \Big\} \\ = - \sum_{i=1}^{\mathtt{n_{el}}} \Big\{ < \mu, t >_{\partial\Omega_i \cap \Gamma_N} + < \mu, g >_{\partial\Omega_i \cap \Gamma_R} \Big\}. \end{aligned} \tag{8}$$

In order to derive the discrete weak forms of the local problem the following discrete spaces are introduced:

$$\begin{aligned} \boldsymbol{\mathcal{W}}^h(\Omega) &= \Big\{ \boldsymbol{w} \in [\mathcal{L}_2(\Omega)]^{\mathtt{n_{sd}}}; \boldsymbol{w}|_{\Omega_i} \in [\mathcal{P}^k(\Omega_i)]^{\mathtt{n_{sd}}} \forall \Omega_i \Big\} && \subset \boldsymbol{\mathcal{W}}(\Omega \\ \mathcal{V}^h(\Omega) &= \Big\{ v \in \mathcal{L}_2(\Omega); v|_{\Omega_i} \in \mathcal{P}^k(\Omega_i) \forall \Omega \Big\} && \subset \mathcal{V}(\Omega), \\ \mathcal{M}^h(S) &= \Big\{ \mu \in \mathcal{L}_2(S); \mu|_{\Gamma_i} \in \mathcal{P}^k(\Gamma_i) \forall \Gamma_i \subset S \subset \Gamma \cup \partial\Omega \Big\} && \subset \mathcal{M}(S), \end{aligned}$$

where $\mathcal{P}^k(\Omega_i)$ and $\mathcal{P}^k(\Gamma_i)$ are the spaces of polynomial functions of degree at most $k \geq 1$ in Ω_i and Γ_i respectively.

With these discrete spaces an element-by-element nodal interpolation of the corresponding variables can be written as

$$\begin{aligned} \boldsymbol{q} \approx \boldsymbol{q}^h &= \sum_{i=1}^{\mathtt{n_{el}}} N_j \mathrm{q}_j && \in \boldsymbol{\mathcal{W}}^h, \\ u \approx u^h &= \sum_{i=1}^{\mathtt{n_{el}}} N_j \mathrm{u}_j && \in \mathcal{V}^h, \\ \hat{u} \approx \hat{u}^h &= \sum_{i=1}^{\mathtt{n_{el}}} \widehat{N}_j \hat{\mathrm{u}}_j && \in \mathcal{M}^h(\Gamma \cup \Gamma_N \cup \Gamma_R) \text{ or } \mathcal{M}^h(\Gamma), \end{aligned}$$

where $\boldsymbol{q}_j$, u_j and $\hat{u}_j$ are nodal values, N_j are polynomial shape functions of order k in each element, $\mathtt{n_{en}}$ is the number of nodes per element, $\widehat{N}_j$ are polynomial shape functions of order k in each element face/edge, and $\mathtt{n_{fn}}$ is the corresponding number of nodes per face/edge.

Replacing the corresponding variables with the given interpolations and using the definitions from [1] the weak form of the local problem (7) can be written in matrix form for each element

Ω_i (i.e., for $i = 1, ..., \mathtt{n_{el}}$) as

$$\begin{bmatrix} \mathbf{A}_{uu} & \mathbf{A}_{uq} \\ \kappa \mathbf{A}_{uq}^T & \mathbf{A}_{qq} \end{bmatrix}_i \begin{Bmatrix} \mathbf{u}_i \\ \mathbf{q}_i \end{Bmatrix} = \begin{Bmatrix} \mathbf{f}_u \\ \kappa \mathbf{f}_q \end{Bmatrix}_i + \begin{bmatrix} \mathbf{A}_{u\hat{u}} \\ \kappa \mathbf{A}_{q\hat{u}} \end{bmatrix}_i \hat{\mathbf{u}}_i.$$

Using the interpolation in the same way for the global problem (8) we get the following system of equations in matrix form:

$$\sum_{i=1}^{\mathtt{n_{el}}} \left\{ [\mathbf{A}_{u\hat{u}}^T \mathbf{A}_{q\hat{u}}^T]_i \begin{bmatrix} \mathbf{u}_i \\ \mathbf{q}_i \end{bmatrix} + [\mathbf{A}_{\hat{\mathbf{u}}\hat{\mathbf{u}}}]_i \hat{\mathbf{u}}_i + [\mathbf{A}_{\hat{\mathbf{u}}\hat{\mathbf{u}}}{}^R]_i \hat{\mathbf{u}}_i \right\} = \sum_{i=1}^{\mathtt{n_{el}}} \left\{ [\mathbf{f}_{\hat{\mathbf{u}}}]_i + [\mathbf{f}_{\hat{\mathbf{u}}}{}^R]_i \right\} \tag{9}$$

Following the notation from [1] the matrices $\mathbf{A}_{\hat{\mathbf{u}}\hat{\mathbf{u}}}{}^R$ and $\mathbf{f}_{\hat{\mathbf{u}}}{}^R$ are defined as follows:

$$\mathbf{A}_{\hat{\mathbf{u}}\hat{\mathbf{u}}}{}^R = - \sum_{\partial\Omega_i \cap \Gamma_R} \gamma \sum_{g=1}^{\mathtt{n_{ip}^f}} \widehat{\mathbf{N}}_{\mathbf{n}}(\xi_{\mathbf{g}}^{\mathbf{f}}) \widehat{\mathbf{N}}^T(\xi_{\mathbf{g}}^{\mathbf{f}}) w_g^f \tag{10}$$

$$\mathbf{f}_{\hat{\mathbf{u}}}{}^R = - \sum_{\partial\Omega_i \cap \Gamma_R} \sum_{g=1}^{\mathtt{n_{ip}^f}} \mathbf{N}(\xi_{\mathbf{g}}^{\mathbf{f}}) g(\mathbf{x}(\xi_{\mathbf{g}}^{\mathbf{f}})) w_g^f \tag{11}$$

Finally, the solution of the local problem (9) is substituted into (11) an can be written as

$$\widehat{\mathbf{K}} \hat{\mathbf{u}} = \hat{\mathbf{f}},$$

where

$$\widehat{\mathbf{K}} = \mathop{\mathbf{A}}_{i=1}^{\mathtt{n_{el}}} [\mathbf{A}_{u\hat{u}}^T \mathbf{A}_{q\hat{u}}^T]_i \begin{bmatrix} \mathbf{A}_{uu} & \mathbf{A}_{uq} \\ \kappa \mathbf{A}_{uq}^T & \mathbf{A}_{qq} \end{bmatrix}_i^{-1} \begin{bmatrix} \mathbf{A}_{u\hat{u}} \\ \kappa \mathbf{A}_{q\hat{u}} \end{bmatrix}_i + \mathbf{A}_{\hat{\mathbf{u}}\hat{\mathbf{u}}}]_i + [\mathbf{A}_{\hat{\mathbf{u}}\hat{\mathbf{u}}}{}^R]_i$$

and

$$\hat{\mathbf{f}} = \mathop{\mathbf{A}}_{i=1}^{\mathtt{n_{el}}} [\mathbf{f}_{\hat{\mathbf{u}}}]_i + [\mathbf{f}_{\hat{\mathbf{u}}}{}^R]_i - [\mathbf{A}_{u\hat{u}}^T \mathbf{A}_{q\hat{u}}^T]_i \begin{bmatrix} \mathbf{A}_{uu} & \mathbf{A}_{uq} \\ \kappa \mathbf{A}_{uq}^T & \mathbf{A}_{qq} \end{bmatrix}_i^{-1} \begin{Bmatrix} \mathbf{f}_u \\ \kappa \mathbf{f}_q \end{Bmatrix}_i.$$

2. Implement in the Matlab code provided in class the corresponding HDG solver.

For the proper implementation of Neumann and Robin boundary conditions several functions of the provided code had to be changed. First of all the numbering of the DOF's in the main and preproscess file was adapted to consider the new boundary conditions. Also the definition of exterior faces, that only accounted for Dirichlet boundary conditions so far, had to be extended for Neumann and Robin accordingly. Furthermore, the assembly of the matrices was adapted to incorporate the new boundaries.

3. Set $\kappa = 9.4$ and $\gamma = 15.9$. Consider $u(x, y) = \sinh ax + by + c \cos \gamma\pi x$ with $a = 0.6$, $b = 0.4$ and $c = -0.5$. Determine the analytical expressions of the data u_D, t and g in Problem (1).

The following analytical expressions for u_D, t, g and for completeness the source term s were determined with the Matlab tools for symbolic calculus:

$$\begin{aligned}
u_D &= \sinh\left(a\,x + b\,y\right) + c\,\cos\left(\pi\,\gamma\,x\right)\\
t &= -\cosh\left(b\,y + a\,x\right)\,b\,k\\
g &= \gamma\,\left(\sinh\left(a\,x + b\,y\right) + c\,\cos\left(\pi\,\gamma\,x\right)\right) - k\,\left(\cosh\left(b\,y + a\,x\right)\,a - \pi\,c\,\sin\left(\pi\,\gamma\,x\right)\,\gamma\right)\\
s &= -k\,\left(a^2\sinh\left(a\,x + b\,y\right) + b^2\sinh\left(a\,x + b\,y\right) - c\,\gamma^2\,\pi^2\,\cos\left(\pi\,\gamma\,x\right)\right).
\end{aligned}$$

4. Solve Problem (1) using HDG with differnet meshes and polynomial degrees of approximation. Starting from the plots provided by the Matlab code, discuss the accuracy of the obtained solution u and of the postprocessed one u^*.

Figure 2 shows the HDG approximation of u and u^* for a mesh with 2048 elements and a polynomial degree $k = 1$. The $\mathcal{L}_2$-norm of the error for u is 7.102307e-01 and respectively 7.699715e-03 for the post-processed HDG solution u^*. Even though the chosen mesh is fine, the error produced by the linear interpolation is relatively high. This inaccuracy is compensated by the post-processed solution, which can reduce the error by a magnitude of two.

When coarsening the mesh, but increasing the polynomial degree k by one, a similar picture emerges. The HDG solution u and the post-processed HDG solution u^* for 512 elements and a polynomial degree $k = 2$ are displayed in Figure 3. The standard HDG solution has an error of 2.549036e-01 and the post-processed result an error of 5.799141e-03. Again, the standard approach fails to represent the analytical solution correctly showing several erroneous parts inside the elements. On the other Hand, the post-processed HDG solution u^* smoothens the result and reduces the error by the order of two. When comparing the analytical solution form Figure 1a with the post-processed HDG solution in Figure 3 differences between the plots are barely visible.

A further increase of the mesh size and a polynomial degree of $k = 3$ leads to the results displayed in Figure 4. The HDG solution produces an error of 7.665966e-01 and the post-processed HDG solution has an error of 2.847956e-02. Similar to the preceding examples, the standard HDG shows artificially large deformations in the corner of the elements, that result in a relatively large error estimate. The post-processed solution is able to smooth and decrease the error, but can not achieve as good results as the preceding solutions due to mesh limitations.

5. Compute the errors for u, $\boldsymbol{q}$ and u^* in the $\mathcal{L}_2$-norm defined on the domain Ω. Perform a convergence study for the primal, u, mixed $\boldsymbol{q}$ and postprocessed, u^* variables for a polynomial degree of approximation $k = 1, .., 4$. Discuss the obtained numerical results, starting from the theoretical results on the optimal convergence rates of HDG.

According to literature the optimal convergence rate of HDG for the approximations of u^h and

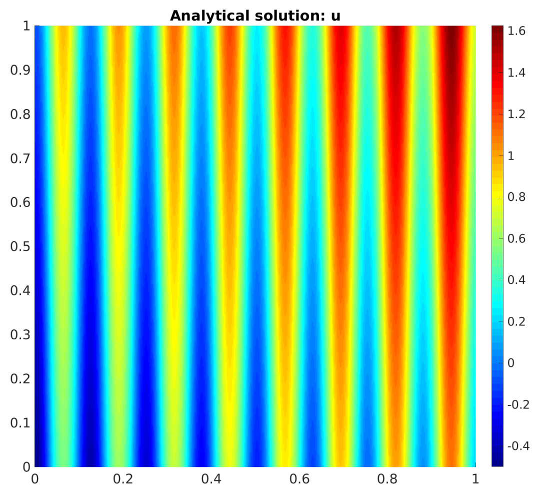

(a) Analytical solution

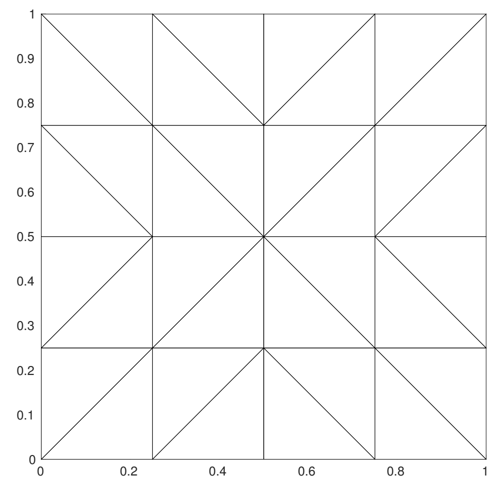

(b) Mesh with element size $h = 0.25$

Figure 1

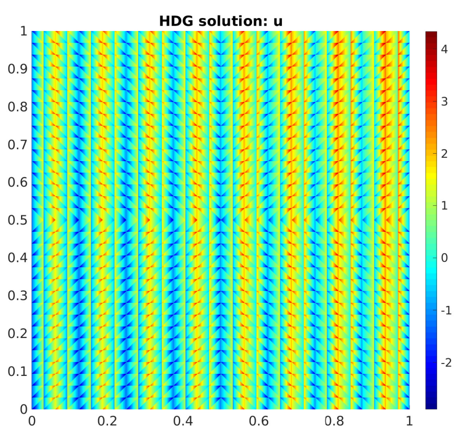

(a) HDG solution

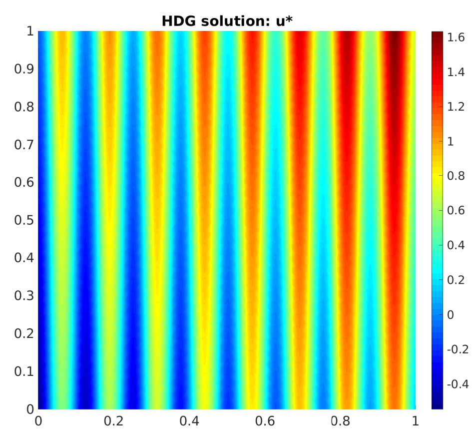

(b) Postprocessed HDG solution

Figure 2: 2048 elements and polynomial degree $k = 1$

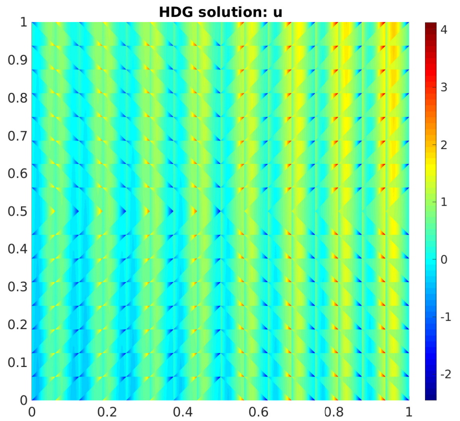

(a) HDG solution

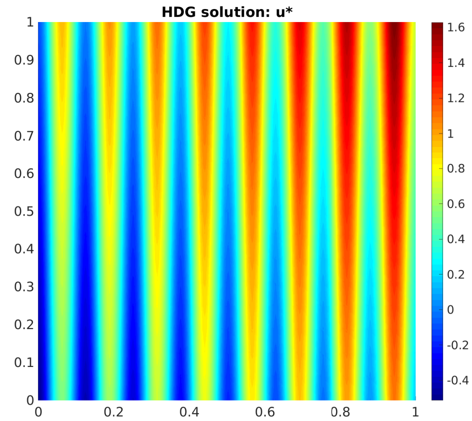

(b) Postprocessed HDG solution

Figure 3: 512 elements and polynomial degree $k = 2$

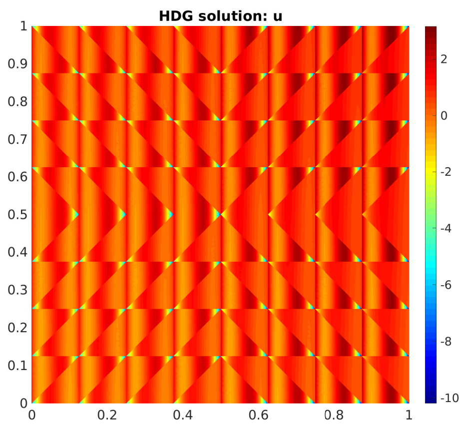

(a) HDG solution

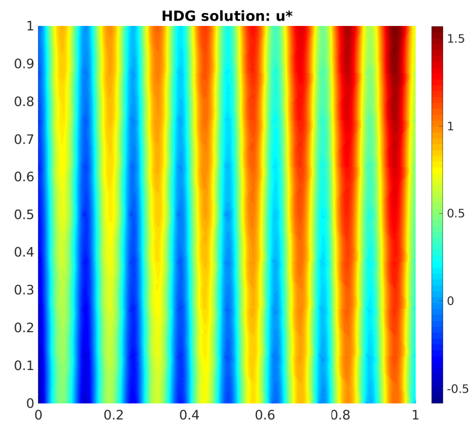

(b) Postprocessed HDG solution

Figure 4: 128 elements and polynomial degree $k = 3$

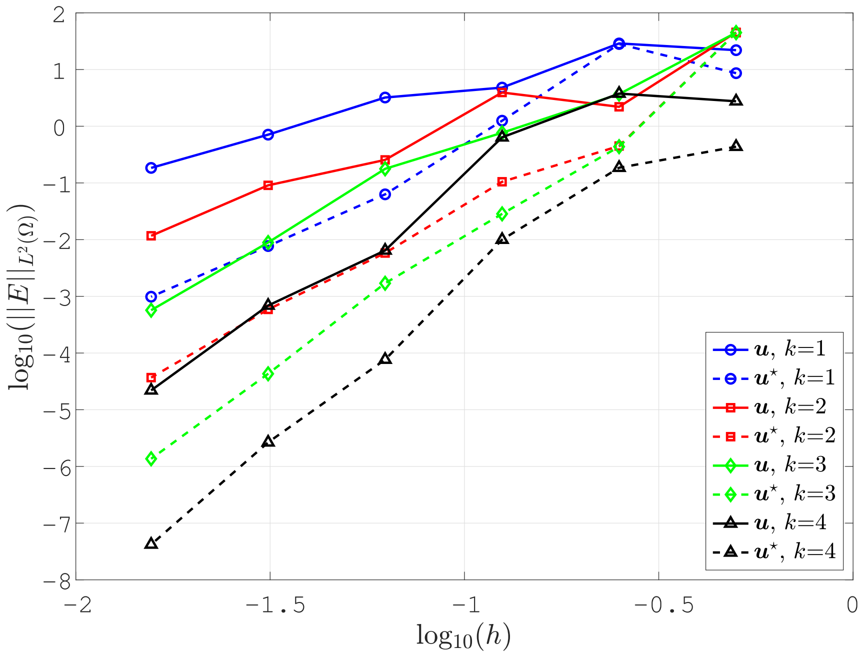

Figure 5: Convergence plot

$\boldsymbol{q}^h$ (here simply denoted as u and $\boldsymbol{q}$) is defined as $k+1$. For the post-processed approximation u^* super-convergent behaviour is expected.

Looking at the convergence plot of u and u^* we can observe that for $k = 1$ and $k = 4$ the error increases for the first mesh refinement. For $k = 2$ this increase also happens at the second mesh refinement. This behaviour can be explained by taking a closer look at Figure 1 with the analytical solution and a mesh representing the second mesh from the convergence study. It is notable that the wave length of the underlying problem is much smaller than the element size in the first two meshes. The fast changes in the gradient of the function can not be represented even for higher polynomial degrees ($k = 4$) and therefore lead to the given error estimates. However, for finer meshes the expected convergence behaviour of HDG method is clearly visible. Both solutions show a similar convergence rate for different polynomial degrees k, but again the post-processed solution u^* shows a much smaller error estimate, roughly by the order of two. These observation coincide with the described theoretical behaviour, at least for small mesh sizes.

References

[1] Sevilla R., Huerta A. (2016) Tutorial on Hybridizable Discontinuous Galerkin (HDG) for Second-Order Elliptic Problems. In: Schröder J., Wriggers P. (eds) *Advanced Finite Element Technologies*. CISM International Centre for Mechanical Sciences (Courses and Lectures), vol 566. Springer, Cham